Volume 55(11): 1129–1137, 2007
Journal of Histochemistry & Cytochemistry
http://www.jhc.org

ARTICLE

Mitochondrial Ferritin Expression in Adult Mouse Tissues

Paolo Santambrogio, Giorgio Biasiotto, Francesca Sanvito, Stefano Olivieri, Paolo Arosio, and Sonia Levi

Department of Bio Technology (SL,PS), Department of Pathology (FS,SO), San Raffaele Scientific Institute, Milan, Italy; Section of Chemistry, Faculty of Medicine, University of Brescia, Brescia, Italy (GB,PA); and Vita-Salute, San Raffaele University, Milan, Italy (SL)

SUMMARY Mitochondrial ferritin (FtMt) is a novel ferritin type specifically targeted to mitochondria. It is highly expressed in the human testis and in sideroblasts from patients with sideroblastic anemia, but other organs have not been studied. To study its expression in the main organs of the mouse, we first used RT-PCR and then produced recombinant mouse FtMt and specific antibodies. Immunohistochemistry analyses confirmed that FtMt is highly expressed in mouse testis, particularly in spermatocytes and interstitial Leydig cells. The protein was also identified in other organs including heart, brain, spinal cord, kidney, and pancreatic islet of Langerhans but not in liver and splenocytes, which have iron storage function and express high levels of cytosolic ferritins. Results indicate that the primary function of ferritin FtMt is not involved in storing cellular or body iron, but its association with cell types characterized by high metabolic activity and oxygen consumption suggests a role in protecting mitochondria from iron-dependent oxidative damage.

(J Histochem Cytochem 55:1129–1137, 2007)

KEY WORDS
mitochondrial ferritin
expression
iron
immunohistochemistry

MITOCHONDRIAL FERRITIN (FtMt) is an iron storage protein belonging to the ferritin family (Levi and Arosio 2004). In human it is encoded by an intronless gene located on chromosome 5q23.1 (Drysdale et al. 2002). The corresponding full-length mRNA has a size similar to that of cytosolic ferritin (~1 kb) but lacks the IRE consensus sequence for iron-dependent translational control (Levi et al. 2001). Thus, FtMt expression is not regulated by IRE/IRP machinery, which controls cellular iron homeostasis (Gebauer and Hentze 2004). FtMt differs from the cytosolic H- (FtH) and L-ferritin chains (FtL) by having a long amino acid N-terminal extension for mitochondrial import, which is cleaved during processing. The sequence of the mature protein is ~79% identical to that of the cytosolic H-ferritin and has ferroxidase activity, but accumulates specifically in the mitochondria forming homopolymers (Levi et al. 2001). Crystallographic data showed that the mature recombinants FtMt and FtH have remarkably similar structures (Langlois d'Estaintot et al. 2004). Recombinant FtMt is an efficient ferritin that readily incorporates and oxidizes iron in vitro, but its rate of ferroxidation is slower than that of FtH (Langlois d'Estaintot et al. 2004; Bou-Abdallah et al. 2005). Studies on HeLa and H1299 cells transfected with the full FtMt cDNA showed that FtMt incorporated iron even more efficiently than the cytosolic ferritins, and its overexpression caused a cellular iron-deficient phenotype (Corsi et al. 2002; Nie et al. 2005). Thus, FtMt attracts iron inside the mitochondria in a non-toxic form. It was also recently shown that FtMt expression inhibited in vivo tumor growth due to cytosolic iron deprivation (Nie et al. 2006). Further studies on a yeast model of Friedreich's ataxia indicated that human FtMt expression reduced the defects caused by frataxin deficiency, including growth inhibition, oxidative damage, and even the level of mitochondrial iron accumulation (Campanella et al. 2004). In human, FtMt mRNA is highly expressed in the testis (Levi et al. 2001), and FtMt protein was found to accumulate in iron-loaded mitochondria of patients with sideroblastic anemia (SA) (Cazzola et al. 2003). FtMt could not be detected in normal erythroid cells, but it is expressed early in the differentiation of the erythroid progenitors of patients with SA (Tehranchi et al. 2005). None of the cultured cell lines from different origins so far analyzed showed

Correspondence to: Prof. Sonia Levi, Vita-Salute, San Raffaele University and San Raffaele Scientific Institute, Via Olgettina 58, 20132 Milan, Italy. E-mail: levi.sonia@hsr.it

Received for publication May 10, 2007; accepted June 25, 2007 [DOI: 10.1369/jhc.7A7273.2007].

0022-1554/07/$3.30

detectable expression of FtMt protein or mRNA. Mitochondrial ferritin was also described in plants (Zancani et al. 2004) and, very recently, in Drosophila (Missirlis et al. 2006). Insect FtMt is encoded by an intron-containing gene indicating a different phylogenetic origin and shows a 42% identity with the human homolog (Missirlis et al. 2006). Transgenic flies overexpressing the fly FtMt did not show evident alterations in iron homeostasis, although female flies had a reduced life span under iron-limiting conditions and were partially protected from paraquat toxicity (Missirlis et al. 2006). FtMt presence in animal and plant species supports the hypothesis that it may be important for mitochondrial iron regulation, but it is unclear whether its primary function is storing iron or scavenging iron excess and toxicity. Detailed data on FtMt expression pattern in mice should provide indications on its functional role.

In this study we describe the characterization of the recombinant mature mouse mitochondrial ferritin (rMoFtMt) that was used to elicit specific antibodies for studying the localization of FtMt protein and quantifying it in adult mouse tissues. Results show that FtMt is expressed in various oxygen-consuming cell types, whereas it is absent or undetectable in tissues that have a major iron storage function. The data support the hypothesis that FtMt has a role in protecting mitochondria from oxidative damage rather than storing iron for the synthesis of mitochondrial iron enzymes.

Materials and Methods

RNA Extraction and RT-PCR

Mouse tissue RNA was extracted by RNAzol B (BIOTECX Laboratories; Houston, TX) and extensively treated with DNase. MoFtMt mRNA was reverse transcribed and amplified by polymerase chain reaction (PCR). cDNA was synthesized from 1 μg total RNA using 250 ng random hexamers with 200 U superscript II (Invitrogen; Milan, Italy) in a final volume of 50 μl. It was then amplified by semi-nested PCR. In the first step the method used primers mFT1F 5′-atgctgtcctgcttttggttc-3′ and mT4R 5′-cagagtatgtaagtccagcag-3′, which generated a fragment of 528 base pair (bp); in the second amplification primers mT1: 5′-tatttccttcgccagtccctg-3′ and mT4R were used, which generated a fragment of 201 bp. Cycling conditions in both amplifications were as follows: 2 min at 94C, 45 cycles (30 sec at 94C, 30 sec at 58C, and 30 sec at 72C), followed by 7 min at 72C. PCR was performed in 50 μl containing the following: 25 pmol of each primer, 1.5 mM $MgCl_2$, 1X PCR buffer (Sigma; Milan, Italy), 200 μM of each dNTPs (Roche; Monza, Italy), and 1 U Taq DNA polymerase (Sigma). Amplification products were then evaluated by electrophoresis. Analyses were run in parallel with controls without reverse transcriptase (RT), which always gave negative results.

Recombinant Ferritin Production and Purification

Cloning, expression, and purification of recombinant mouse ferritin H- and L-chains were described by Santambrogio et al. (2000). cDNA encoding the mature mouse mitochondrial ferritin protein (aa 57–237) was obtained with reverse transcription by 1 μg of testis total RNA using SuperScript II Reverse Transcriptase (Gibco; Gaithersburg, MD) and was cloned into the pET expression vector (Novagen-EMD Biosciences; Madison, WI) (pET-MoMtF) in NdeI and BamHI sites. The plasmid was used to transform BL21DE3 *Escherichia coli* strain, the transformed cells were grown in LB broth at 37C until reaching optical density of 0.7 at 650 nm, expression was then induced by the addition of 1 mM IPTG, and the cells were grown for an additional 3 hr. Harvested cells were disrupted by sonication, and the soluble homogenate was heated at 75C for 10 min, precipitated with 520 g/liter of ammonium sulfate, and treated with DNase and RNase. Further purification of the protein consisted of gel filtration on a Sepharose 6B (Amersham-GE Healthcare; Milano, Italy) column followed by ion-exchange chromatography on HiTrap Q (Amersham). MoFtMt was judged >95% pure by gel electrophoresis. Protein concentration was determined by BCA method (Pierce Biotechnology; Rockford, IL) using BSA as standard.

Iron Incorporation

Apoferritins were prepared by incubation with 1% (v/v) thioglycolic acid (pH 5.5) and 2,2-bipyridine followed by dialysis against 0.1 M Hepes buffer, pH 7.0. Apoferritins (1 μM, 0.5 mg/ml) were diluted in 0.1 M Hepes buffer, pH 7.0, and incubated for 2 hr at room temperature with 1 mM of freshly made ferrous ammonium sulfate.

Analytical Methods

Non-denaturing electrophoreses were carried out on 6% polyacrylamide gels. Separated ferritins were revealed by staining with Coomassie blue or Prussian blue or transferred to nitrocellulose filter for immunoblotting. SDS-PAGE was performed on 15% polyacrylamide gel, and proteins were stained by Coomassie blue or transferred to nitrocellulose filter.

Antibody Production

Antibodies specific for the cytosolic forms of mouse ferritin were obtained according to Santambrogio et al. (2000). To obtain antibodies specific for MoFtMt, New Zealand White rabbits were immunized on day 0 with 200 μg of purified mature recombinant MoFtMt (residues 57–237) emulsified with complete Freund's adjuvant. Two additional booster doses of 200 μg of MoFtMt emulsified with incomplete Freund's adjuvant were injected SC on day 10 and on day 20. Antisera IgG were partially purified by ammonium sulfate precipitation (50% saturation) prior to labeling with horseradish peroxidase (HRP).

Tissue Preparation

C57/B6 mice were obtained from exceeding control group animals in the animal facility of our institution. Mouse tissue was dissected according to approved protocols. Freshly dissected tissues were either frozen in liquid nitrogen or fixed in 10% formaldehyde and embedded in paraffin for immunohistochemical studies or minced and lysed in ice-cold lysis buffer (20 mM Tris buffer, pH 7.4, 1% Triton X-100, 1 mM Na azide, 1 mM PMSF, 10 μM leupeptin, 1 μM pepstatin) in

Potter homogenizer or stored at −80C prior to preparation of homogenates. The homogenate was clarified by centrifugation at 10,000 × g for 10 min at 4C, and the supernatant was used in Western blotting or in ELISA experiments. Mitochondrial-enriched preparations from tissues were obtained by standard procedure. Freshly obtained mouse tissues were minced and lysed in ice-cold lysis buffer (5 mM Tris buffer, pH 7.4, 250 mM sucrose, 0.1 mM PMSF) in Potter homogenizer and centrifuged at 600 × g for 15 min at 4C to remove nuclei and cell debris. The soluble fraction was further centrifuged at 10,000 × g for 25 min at 4C, the supernatant was used as cytosolic fraction, and the pellet was dissolved in the same buffer containing 1 mM EDTA and spun at 10,000 × g for 25 min at 4C. The mitochondrial pellet was washed with the same buffer and then dissolved in PBS containing 0.007% digitonin and left 20 min in ice. Mitoplasts were recovered by centrifugation at 10,000 × g for 10 min at 4C and lysed in 20 mM Tris buffer, pH 7.4, 0.5% Triton X-100, 0.1 mM PMSF, clarified at 10,000 × g for 10 min at 4C, and used for Western blotting experiments.

Immunological Methods

Western Blotting. Nitrocellulose filters were incubated with the antibody specific for the mitochondrial ferritin (1:5000 dilution) or for the cytosolic ferritin (1:2000 dilution) for 1 hr at room temperature and then with the secondary HRP-labeled anti-rabbit IgG antibody for 1 hr at room temperature. Chemiluminescent signal was developed by ECL Advance (Amersham).

ELISA Assays. The method for quantification of ferritins with antibodies specific for the cytosolic ferritin H- or L-chains was described previously (Santambrogio et al. 2000). Quantification of mitochondrial ferritin was determined by the following specific ELISA assay. Microtiter plates were coated with 1 μg of polyclonal antibodies specific for the MoFtMt. Standard FtMt or samples were added to the plates, incubated for 1 hr at 37C, washed, and further incubated for 1 hr with the same antibodies labeled with HRP to reveal the bound ferritin. Activity was developed with *o*-phenylenediamine dihydrochloride (Sigma).

Immunohistochemistry

Four-μm sections were prepared from formalin-fixed, paraffin-embedded murine tissues, deparaffinized in xylene, and rehydrated in graded alcohol. Immunolocalization for mouse mithocondrial ferrritin was carried out after antigen retrieval by 0.05% protease type XIV digestion for 5 min at 37C, quenching of endogenous peroxidase in 3% H_2O_2, and blocking in 5% normal goat serum 30 min at room temperature. Sections were sequentially incubated with the polyclonal rabbit αMoFtMt antibody (1:700 dilution) for 2 hr at room temperature and with 1:200 dilution of peroxidase-labeled polymer conjugated to goat α-rabbit immunoglobulins (DAKO EnVision+ System; Dako, Milano, Italy) for 30 min at room temperature. Immunoreaction was revealed by HRP using 3,3′-diaminobenzidine as chromogen (Biogenex; San Ramon, CA) for 5 min at room temperature, and the slides were slightly counterstained with Harris' hematoxylin. For some tissues (i.e., pancreas), the experiment was carried out on 5-μm cryosections, fixed with 4% paraformaldehyde for 10 min at room temperature, and treated with 1% Triton X-100 for 15 min before incubation with the polyclonal rabbit anti-FtMt antibody as described above. In control experiments, anti-FtMt antiserum was preabsorbed overnight at 4C with an excess of antigen (final concentration ∼0.25 mg/ml) or it was omitted. Immunolocalization for H- and L-ferritin on murine tissues was performed as above, treating sections previously with microwave retrieval in citrate buffer (pH 6) and using the polyclonal anti H- and anti-L antibody at 1:500 dilution for 16 hr at 4C.

Results

Mammalian FtMt Sequence

Uninterrupted open reading frames encoding ferritins with an N-terminal extension were found in mammalian but not in other vertebrate genomes. Sequences of the predicated mature FtMt from different mammalian species are highly conserved with identities >80% (Figure 1). The N-terminal sequences have a similar length; all have a high probability to act as efficient mitochondrial exporters ($p>0.87$) and to be cleaved in overlapping sites, although they are more divergent. Drosophila FtMt has a shorter leader sequence of 13 amino acids, which is predicted to be efficient in mitochondria targeting ($p=0.87$). In the completed mammalian genomes, FtMt is located in conserved sequences, being flanked by PRR16 and SRFBP1 genes (UCSC Genome Browser database). Conservation of the sequence and of the genetic localization supports the hypothesis that they are similarly regulated and have analogous functions in the various species.

Expression of MoFtMt in Mouse Tissues

As a first approach to study MoFtMt expression pattern, we used the sensitive RT-PCR method on a panel of mouse tissues. This showed high levels of MoFtMt mRNA only in testis, whereas lower levels were present in brain, kidney, heart, thymus, and spleen (Figure 2). High mRNA levels were also found in mouse embryos from day E12.5 to E17.5 (not shown). These data stimulated the study of FtMt protein expression in various adult tissues.

Characterization of Recombinant Mouse Mitochondrial Ferritin and of Its Antibody

Recombinant mature mitochondrial ferritin (rMoFtMt) was efficiently expressed in *E. coli*. The protein retained the typical thermal stability of ferritins and was purified with the method developed for cytosolic ferritin (Santambrogio et al. 2000). Non-denaturing PAGE analysis showed that the purified protein had a mobility similar to the recombinant mouse H-ferritin, indicating that it was assembled in the 24-mer shell (Figure 3A, protein); moreover, after aerobic incubation with ferrous iron it formed iron cores positive to Prussian

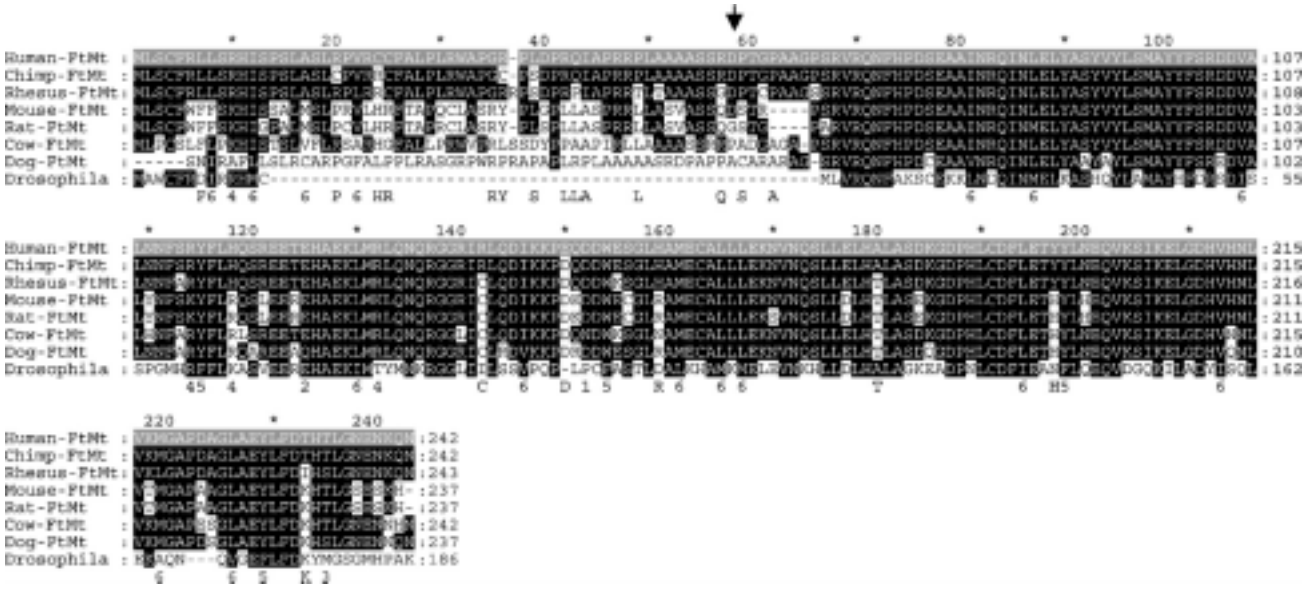

Figure 1 Alignment of FtMt proteins from indicated different species. The conserved amino acids compared with human sequence have a black background. Arrow indicates the putative cleavage site of MoFtMt leader peptide.

blue stain (Figure 3A, iron). Thus, rMoFtMt behaved similarly to human FtMt. The purified protein was used to elicit antisera in rabbit (αMoFtMt), which were tested for specificity. In Western blotting of non-denaturing PAGE (Figure 3A, WB) and SDS-PAGE (not shown), it recognized only rMoFtMt. As observed with previous anti-ferritin antibodies, the binding affinity was higher for native than denatured ferritins (not shown).

To further validate antibody specificity and sensitivity, we analyzed total soluble homogenates from mouse testis, heart, and heart mitochondrial fraction by Western blotting, after separation on non-denaturing PAGE. αMoFtMt recognized the control MoFtMt and a band in the testis and mitochondrial heart samples (Figure 3B, Lanes 1–3), whereas no band was revealed in total heart extract (Figure 3B, Lane 4). The anti-MoFtH antibody recognized a slower-running cytosolic ferritin in total testis and heart homogenates (Figure 3B, Lanes 5 and 6) with only a minor contamination in the heart mitochondrial fraction (Figure 3B, Lane 7).

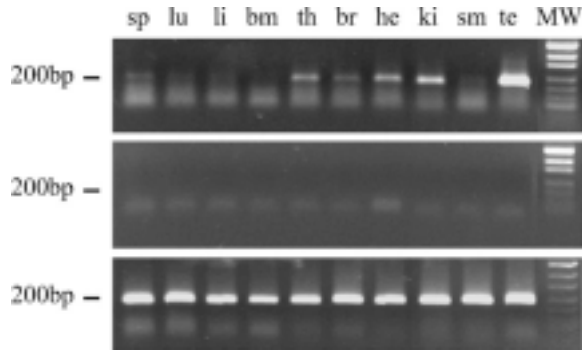

Figure 2 RT-PCR analysis of FtMt mRNA expression in adult mouse tissues. Top panel: RT-PCR analysis of equal amounts of RNA from different mouse organs with primers that produced the indicated specific 200-base pair (bp) DNA fragment. Middle panel: as above but without reverse transcriptase treatment. Lower panel: RT-PCR using primers for housekeeping glyceraldehyde phosphate dehydrogenase mRNA (GAPDH), which produced a 200-bp DNA for control of sample loading and RNA integrity. Lane 1: spleen (sp); Lane 2: lung (lu); Lane 3: liver (li); Lane 4: bone marrow (bm); Lane 5: thymus (th); Lane 6: brain (br); Lane 7: heart (he); Lane 8: kidney (ki); Lane 9: skeletal muscle (sm); Lane 10: testis (te); Lane 11: molecular weight (MW).

Quantification of MoFtMt by ELISA Assay

ELISA assays developed with the αMoFtMt antibody resulted highly specific for MoFtMt, with a sensitivity of 0.25 ng/ml, a linearity between 4 and 500 ng/ml, and no cross-reactivity for the cytosolic FtH and FtL up to 16 μg/ml (not shown). Despite their sensitivity, the assays could not detect MoFtMt in total homogenates from mouse liver, spleen, brain, and the other tissues tested except testis (53 ± 7 ng/mg of total protein) and epididymis (10 ± 3 ng/mg of total protein). It should be noted that FtMt level in testis is comparable to that of L-ferritin content in all the tissues (12–100 ng/mg of total protein) except liver and spleen that have iron storage functions and higher ferritin levels.

Immunohistochemistry on Adult Mouse Testis

We initially used mouse testis slices to set up immunohistochemical methods for MoFtMt detection. Anti-MoFtMt gave a strong signal in interstitial cells, particularly in Leydig cells, and in germinal cells of

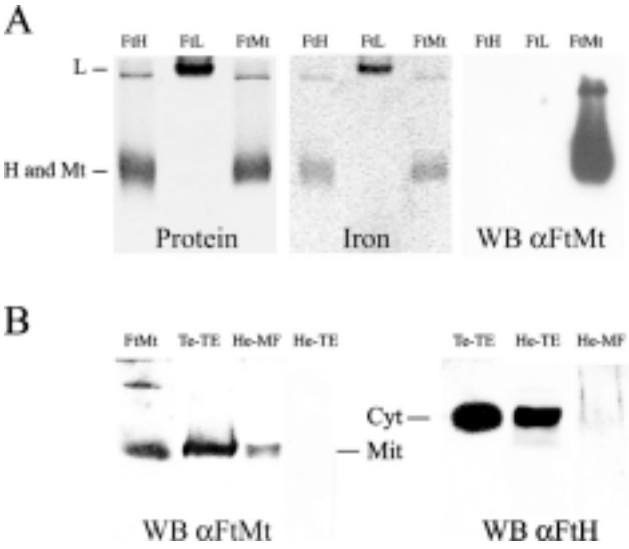

Figure 3 Characterization of rMoFtMt and its rabbit antiserum. (**A**) Purified recombinant mouse H (FtH), L (FtL), and mitochondrial ferritin (FtMt) were separated on non-denaturing PAGE (3 μg of protein per well) and stained for protein with Coomassie blue (Protein) and for iron content with Perl's reagent (Iron), as indicated. A lower load (50 ng of protein per well) was used in Western blotting with anti-MoFtMt antibody (WB αFtMt) as indicated. Mobility of rMoLF (L), rMoHF (H), and rMoFtMt (Mt) is indicated. (**B**) Total soluble extract from mouse testis (Te-TE, 20 μg protein), mitochondrial fraction from heart (He-MF, 20 μg protein), and total soluble extract from heart (He-TE, 20 μg protein) were run on non-denaturing PAGE with recombinant MoFtMt (FtMt, 10 ng) and blotted with the anti-MoFtMt antibody (WB αFtMt). In parallel, total soluble extract from testis (Te-TE, 20 μg), heart (He-TE, 20 μg), and mitochondrial fraction from heart (He-MF, 20 μg protein) were run and blotted with anti mouse H-ferritin antibody (WB αFtH). Mobility of cytosolic (Cyt) and mitochondrial (Mit) ferritins is indicated.

the seminiferous tubule with increasing signal from spermatogonia to spermatozoa (Figure 4A). Controls without the primary antibody (not shown) or after preabsorbing it with rMoFtMt (Figure 4B) were negative, confirming its specificity. This was further supported by the use of other anti-ferritin antibodies: the one for mouse L-ferritin strongly stained only interstitial Leydig cells (Figure 4C), and that for mouse H-ferritin stained Leydig cells and, more weakly, immature germinal cells in the tubule (Figure 4D).

Immunohistochemistry on Adult Mouse Tissues

Immunohistochemical analysis was extended to other adult mouse tissues. Results are summarized in Table 1. Negative staining for FtMt was found in tissues such as prostate, uterus, urinary bladder, seminal vesicles, esophagus, gut, skin, and unexpectedly liver, which is strongly positive for cytosolic L- and H-ferritins. Positive staining in most other tissues was in selected cell types. In the spleen, scattered cells in red pulp with dendritic-like morphology were positive, whereas lymphocytes were negative (Table 1). In the ovary, the cytoplasm of the oocytes was nicely stained for FtMt. On the contrary, the theca layers, granulose, and stromal cells were negative. FtMt was also localized in the ciliated cells of the respiratory epithelium in the lung as well as the epididymis and Fallopian tubes and in the deeper portion of glands in the atrial zone of the stomach (Table 1).

In brain cortex and spinal cord, the antibody stained most, if not all, neurons, whereas glial cells were negative (Figure 5A). Cerebellum showed a strong stain only in the Purkinje cells and in scattered glial cells of the molecular and granular layers (Figure 5B). In the retina, the antibody selectively stained the extension of photoreceptors (inner segment), the outer plexiform layer (where synapses between bipolar, horizontal cells, and photoreceptors occur), and the inner plexiform layer that contains axons and dendrites of amacrine, bipolar, and ganglion cells (Figure 5C). This particular pattern of expression in the retina corresponds to mitochondria-rich cell layers and is typical for mitochondrial proteins.

All cardiac muscle fibers were positively stained (Figure 5D). Higher magnification showed granular staining typical of a mitochondrial-localized protein (Figure 5D, inset). In the kidney, staining was evident in the cells of proximal tubules, in particular in the apical portion, whereas distal tubules and glomeruli were negative (Figure 5E). In pancreas, only the endocrine glands, the islets of Langerhans, were weakly positive, whereas the exocrine portion was negative (Figure 5F). Frozen pancreatic sections analyzed at high magnification showed a granular stain (Figure 5F, inset). In the thymus, the subcapsular and medullary epithelial cells were immunoreactive, whereas thymocytes and macrophages were negative (Figure 5G).

Discussion

The study of FtMt expression pattern in an animal is important to characterize the mechanisms of its cellular expression and to clarify its in vivo physiological role in complement with cellular studies (Corsi et al. 2002; Cazzola et al. 2003; Nie et al. 2005). For this purpose we produced the specific reagents to analyze FtMt in mouse tissues. Recombinant mouse FtMt is similar to, but antigenically distinct from, the human counterpart, and the rabbit antibody that it elicited resulted specific for MoFtMt with negligible cross-reactivity with the cytosolic H/L ferritins. Western blotting and ELISA analyses of total mouse tissue homogenates showed that FtMt is expressed at low levels and is detectable only in a few tissue types (e.g., testis) or in mitochondria-enriched specimens. This is in agreement with RT-PCR assays that showed a high amount of FtMt transcript only in testis. We concluded that blot-

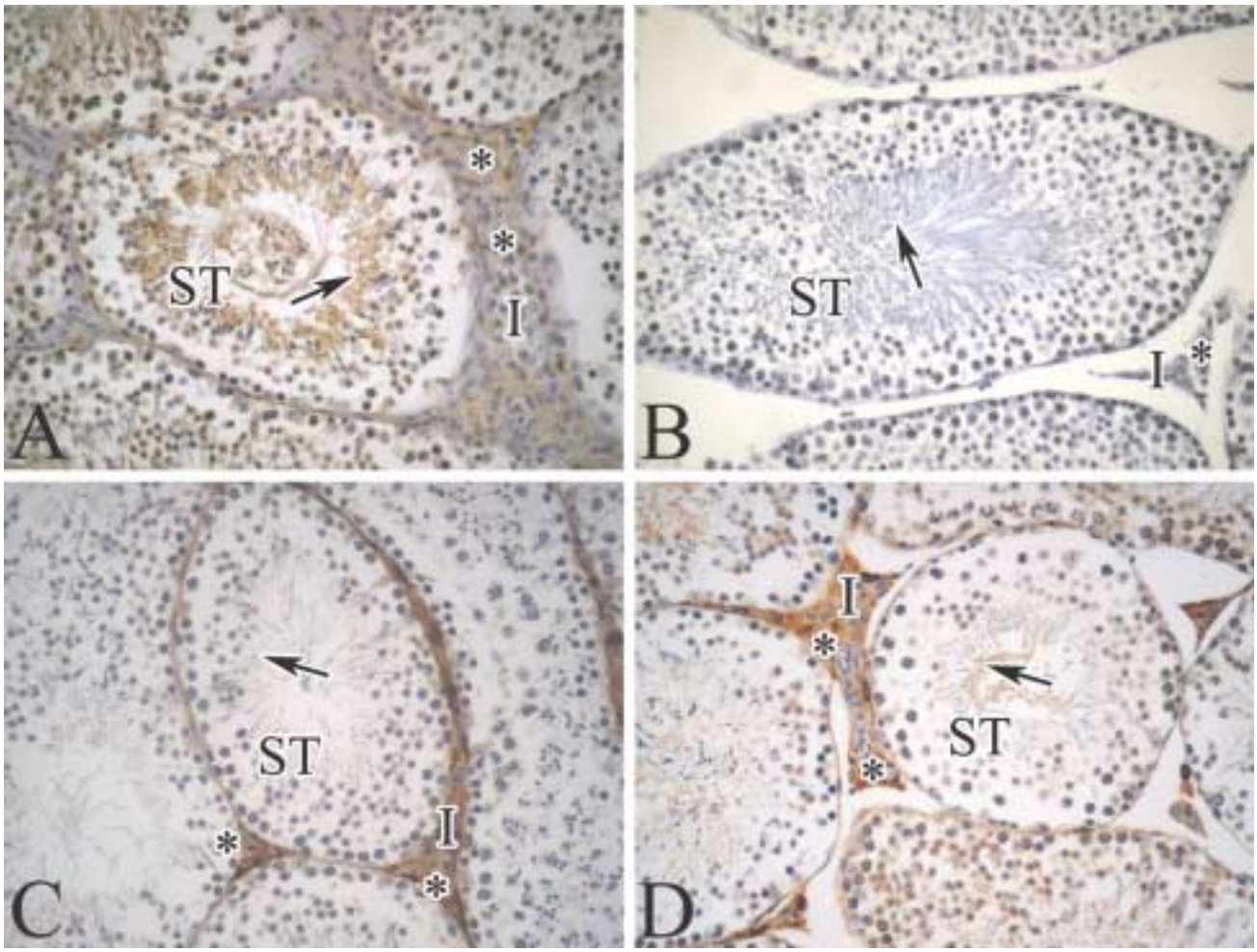

Figure 4 Immunohistochemistry of mitochondrial and cytosolic ferritins in mouse testis. Parallel paraffin-fixed sections of mouse testis were probed with antibodies specific for mouse FtMt (**A**), for cytosolic L- (**C**), and for cytosolic H-ferritin (**D**) or with preabsorbed αMoFtMt antibody (**B**). (**A**) αMoFtMt gave a strong stain of interstitial Leydig cells and of germinal cells, in particular the more mature spermatozoa in the lumen of seminiferous tubules. (**B**) The αMoFtMt antibody preabsorbed with purified recombinant FtMt did not show evident staining, assessing the specificity of the antibody. (**C**) Anti-cytosolic ferritin L-chain stained only interstitial Leydig cells. (**D**) Anti-cytosolic ferritin H-chain stained the interstitial Leydig cells and immature cells of the seminiferous tubules. ST, seminiferous tubules; I, interstitium; asterisk, interstitial Leydig cells; arrow, spermatozoa.

ting and ELISA are not sensitive enough for screening of FtMt expression in tissues.

Immunohistochemistry, which identifies isolated FtMt-expressing cells, gave a more detailed pattern. First, it supported the mitochondrial localization of FtMt. For example, the granular staining of the islets of Langerhans at high magnification is compatible with mitochondrial staining. Moreover, FtMt positivity in the retina was confined to the mitochondria-rich layers (inner segment and outer and inner plexiform layers) as previously described (Hahn et al. 2004). Interestingly, the pattern of expression in the retina is remarkably similar to the one observed for pantothenate kinase 2 (Pank2), a mitochondrial protein involved in neurodegenerative diseases (Kuo et al. 2005), further suggesting the mitochondrial localization of the stain observed with our antibody. However, future ultrastructural studies will be needed to confirm the mitochondria localization of the protein in vivo.

At variance with the cytosolic H- and L-ferritins that are ubiquitous, FtMt is not. Notably, it is virtually absent in liver and, except for a few dendritic-like cells, also in spleen, which are the organs particularly rich in cytosolic H/L ferritins and devoted to iron deposition and management. This strongly indicates that FtMt has no major role in controlling iron homeostasis, and that its expression is not related to iron availability, consistent with the absence of a functional IRE sequence.

A high metabolic rate seems to be a common characteristic of the cells positive to FtMt. For example, FtMt-rich Leydig cells in the testis require a high level of energy for biosynthesis of hormones, and in the semi-

Table 1 FtMt expression in adult mouse tissues

Tissue[a]	Cell type or tissue component	FtMt immunoreactivity[b]
Liver	Hepatocytes	−
Spleen	Dendritic-like cells	+ (scattered)
	Lymphocytes	−
Brain (Figure 5A)	Neuronal cells	+
	Glial cells	−
Cerebellum (Figure 5B)	Purkinje cells	+
Spinal cord	Ganglion cells	+
Eye (Figure 5C)	Retina	+
	Corneal epithelium	+
Heart (Figure 5D)	Myocytes	+
	Interstitial cells	+
Thymus (Figure 5G)	Medullary and subcapsular epithelial cells	+
	Thymocytes	−
	Macrophages	−
Pancreas (Figure 5F)	Endocrine cells	+ (weak)
	Exocrine cells	−
Kidney (Figure 5E)	Proximal tubules	+
	Distal tubules	−
	Glomerulus	−
Testis (Figure 4A)	Leydig cells	+
	Sertoli cells	−
	Spermatogonia/ spermatozoa	+
Epididymis	Epithelium	+
Seminal vesicles		−
Prostate		−
Urinary bladder		−
Ovary	Oocyte	+
	Granulosa cells	−
	Theca layers	−
Fallopian tubes	Epithelium	+
	Stromal cells	−
Uterus		−
Lung	Bronchial epithelium	+ (weak)
Stomach	Deep glandular cells of the antral zone	+
Esophagus		−
Gut		−
Skin		−

[a]Tissues were analyzed in this study by immunohistochemistry using anti-mouse FtMt antibody. Corresponding figures are reported in brackets.
[b]Immunoreactivity is indicated by (+), negative by (−), (scattered) indicates only few positive cells, and (weak) indicates a faint signal.

niferous tubules the germinal cells with highest FtMt content were the more mature spermatozoa in the tail region that lay freely in the lumen. Mitochondria of spermatozoa are highly active in order to meet the requirements for energy-dependent movement, but there are few of them (<100 per cell), implying that the local FtMt concentration in these organelles is very high. These cells are exposed to an oxygen tension much higher than that of other internal cells, and FtMt might offer further protection against oxidative damage. Of interest is that Pank2 is also highly expressed in the spematocytes and Purkinje cells. Although its relationship with iron is unclear, mutations of its gene are associated with brain iron accumulation and also with azoospermia (Kuo et al. 2005).

Another example was the pancreas where FtMt positivity was restricted to the islets of Langerhans, the endocrine cells subjected to highly active metabolism. The epithelia lining the bronchus, the Fallopian tubes, and the epididymis are also FtMt rich, all tissues mostly composed of ciliated cells that use high energy for motility/transport or absorption/phagocytosis. Other tissues with epithelial cells but lacking these functions were not positive for FtMt (Table 1). FtMt localized in the proximal tubules of the kidney where extensive reabsorption of some components of the glomerular filtrate occurs and energy is needed to support ion-pumping epithelial cells. In the thymus, the epitheliocytes, which eliminate immature T-cells recognizing self-antigens and promote differentiation/proliferation/maturation of T-cell, expressed the mitochondrial ferritin. Neurons in the brain cortex and in the spinal cord and neuronal extensions in the retina showed strong reactivity for FtMt, as appeared in all cardiac muscle cells. Maintenance of high metabolic activity is required in neurons to develop electrochemical gradients and in heart to ensure pumping action via rhythmic contraction dependent on Ca^{2+}-ATPase membrane pumps. Furthermore, FtMt was never detected in surface epithelia, which function as a mechanical barrier. Together these data indicate an association of FtMt expression with high cellular metabolic activity and oxygen consumption. Exceptions are the hepatocytes, which are rich in mitochondria and highly metabolically active but negative for FtMt stain. Thus, there was not a simple correlation between the level of FtMt and the number of mitochondria per cell and high-energy cell requirement. FtMt expression appears to better correlate with the necessity of some cell types to manage ATP burst in a short time. This specific high-energy requirement is associated with the production of reactive oxygen species (ROS) derived from the Fenton reaction that involves the Fe(II)-catalyzed production of the highly toxic hydroxyl radicals from hydrogen peroxide. Expression of FtMt may be a cell response to avoid this harmful reaction. This hypothesis is supported by the study of FtMt in *Drosophila melanogaster*, which is also highly expressed in the testis. FtMt overexpression in a fly transgenic model did not have major effects on iron homeostasis but protected female flies against paraquat toxicity, indicating that it may limit free radical generation (Missirlis et al. 2006). Thus, FtMt seems to have the primary role of iron detoxification, but when expressed at high levels it may store iron in the mitochondrial compartment that is not easily accessible. The consequent cellular iron deprivation may be negative for most cells with high iron requirements, particularly the proliferating ones (Nie et al. 2006). This may explain why

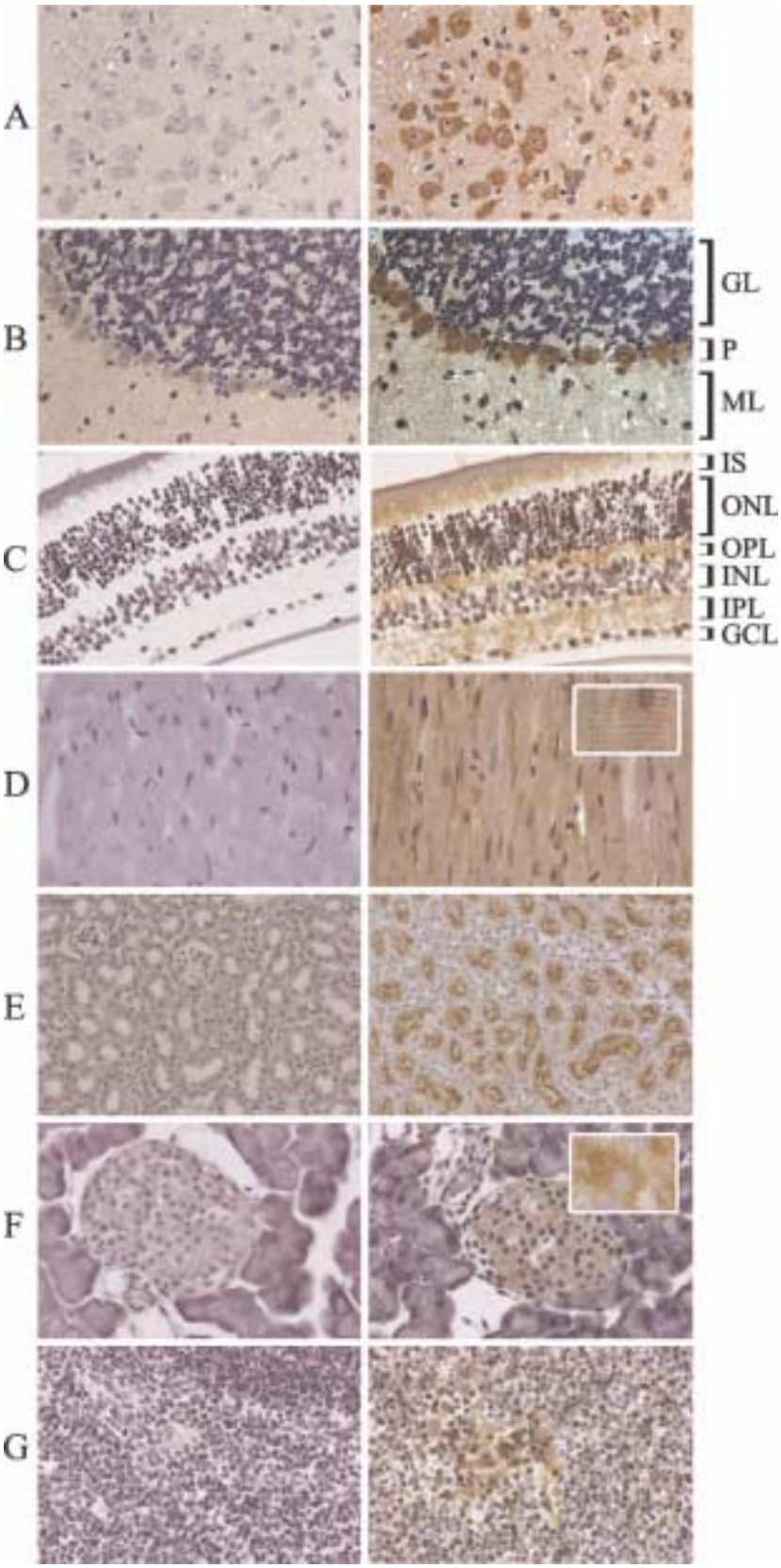

Figure 5 Immunohistochemistry of FtMt in different mouse tissues. Paraffin-fixed sections from the indicated mouse tissues were probed with the anti-FtMt antibody, before (right panels) or after (left panels) preabsorption with rMoFtMt. (**A**) Cerebral cortex showing intense positivity of neuronal cells. (**B**) Positive staining in Purkinje cells in cerebellum. The granular layer (GL), Purkinje cells (P), and molecular layer (ML) are indicated. (**C**) Section of the retina showing staining of the extension of photoreceptors, outer plexiform layer, axons, and dendrites of the ganglion cells in the retina. Inner segments (IS), outer nuclear layer (ONL), outer plexiform layer (OPL), inner nuclear layer (INL), inner plexiform layer (IPL), and ganglion cell layer (GCL) are indicated. (**D**) Heart section with abundant stain of myocytes. Digital zoom of the image shows a granular staining (inset). (**E**) Kidney section showing a strongly positive stain of the cellular apical portion of proximal tubules. (**F**) Frozen section of pancreas showing positivity only in endocrine islet of Langerhans. High magnification showing granular staining (inset). (**G**) Thymus section with positivity in epithelial cells of the medulla.

FtMt is not ubiquitous. In contrast, the easier reutilization and recycling of iron bound to the cytosolic H/L ferritins allow them to act as essential buffers that control, detoxify, and store cellular iron (Harrison and Arosio 1996). Our work seems to indicate that FtMt is required mainly in non-proliferating oxygen-consuming cell types where its iron detoxification properties are needed to reduce ROS toxicity. However, we cannot exclude that it might also be expressed in other cell types at levels below the detection limits of our assays.

An interesting parallelism is found with neuroglobin, which is a cytosolic protein with an expression pattern similar to that of FtMt. It is found in neurons, retina, endocrine tissues, and in the testis (Hankeln et al. 2004; Li et al. 2006). The original hypothesis that it may play a role as O_2 suppliers in condition of hypoxia has not been supported, and it was proposed that its major function is to scavenge ROS and to sustain cellular energy metabolism (Fordel et al. 2007). In addition, its protective action against ischemia (Hundahl et al. 2005) involved the expression of eNOS, which is a regulator of mitochondria functionality (Nisoli et al. 2003; Valerio et al. 2006). This raises the possibility that the two proteins act to limit the damages caused by ROS production in oxygen-consuming cells: FtMt by reducing mitochondrial reactive iron and neuroglobin by scavenging free radicals. Thus, FtMt might belong to the set of proteins dedicated to protect mitochondria and cells from oxidative damage. In conclusion, FtMt expression is tightly regulated and cell specific, and we suggest that its physiological role is associated with the protection of the cell from iron-dependent oxidative damage.

Acknowledgments

This work was partially supported by Telethon–Italy Grant GP0075Y01 (to SL) and by Ministero dell'Università e della Ricerca Scientifica e Tecnologica PRIN 2006 (to SL and PA).

We thank Dr. Claudio Doglioni for helpful suggestions and Martina Rocchi for technical assistance.

Literature Cited

Bou-Abdallah F, Santambrogio P, Levi S, Arosio P, Chasteen ND (2005) Unique iron binding and oxidation properties of human mitochondrial ferritin: a comparative analysis with human H-chain ferritin. J Mol Biol 347:543–554

Campanella A, Isaya G, O'Neill HA, Santambrogio P, Cozzi A, Arosio P, Levi S (2004) The expression of human mitochondrial ferritin rescues respiratory function in frataxin-deficient yeast. Hum Mol Genet 13:2279–2288

Cazzola M, Invernizzi R, Bergamaschi G, Levi S, Corsi B, Travaglino E, Rolandi V, et al. (2003) Mitochondrial ferritin expression in erythroid cells from patients with sideroblastic anemia. Blood 101: 1996–2000

Corsi B, Cozzi A, Arosio P, Drysdale J, Santambrogio P, Campanella A, Biasiotto G, et al. (2002) Human mitochondrial ferritin expressed in HeLa cells incorporates iron and affects cellular iron metabolism. J Biol Chem 277:22430–22437

Drysdale J, Arosio P, Invernizzi R, Cazzola M, Volz A, Corsi B, Biasiotto G, et al. (2002) Mitochondrial ferritin: a new player in iron metabolism. Blood Cells Mol Dis 29:376–383

Fordel E, Thijs L, Moens L, Dewilde S (2007) Neuroglobin and cytoglobin expression in mice. Evidence for a correlation with reactive oxygen species scavenging. FEBS J 274:1312–1317

Gebauer F, Hentze MW (2004) Molecular mechanisms of translational control. Nat Rev Mol Cell Biol 5:827–835

Hahn P, Dentchev T, Qian Y, Rouault T, Harris ZL, Dunaief JL (2004) Immunolocalization and regulation of iron handling proteins ferritin and ferroportin in the retina. Mol Vis 10:598–607

Hankeln T, Wystub S, Laufs T, Schmidt M, Gerlach F, Saaler-Reinhardt S, Reuss S, et al. (2004) The cellular and subcellular localization of neuroglobin and cytoglobin—a clue to their function? IUBMB Life 56:671–679

Harrison PM, Arosio P (1996) The ferritins: molecular properties, iron storage function and cellular regulation. Biochim Biophys Acta 1275:161–203

Hundahl C, Stoltenberg M, Fago A, Weber RE, Dewilde S, Fordel E, Danscher G (2005) Effects of short-term hypoxia on neuroglobin levels and localization in mouse brain tissues. Neuropathol Appl Neurobiol 31:610–617

Kuo YM, Duncan JL, Westaway SK, Yang H, Nune G, Xu EY, Hayflick SJ, et al. (2005) Deficiency of pantothenate kinase 2 (Pank2) in mice leads to retinal degeneration and azoospermia. Hum Mol Genet 14:49–57

Langlois d'Estaintot B, Santambrogio P, Granier T, Gallois B, Chevalier JM, Precigoux G, Levi S, et al. (2004) Crystal structure and biochemical properties of the human mitochondrial ferritin and its mutant Ser144Ala. J Mol Biol 340:277–293

Levi S, Arosio P (2004) Mitochondrial ferritin. Int J Biochem Cell Biol 36:1887–1889

Levi S, Corsi B, Bosisio M, Invernizzi R, Volz A, Sanford D, Arosio P, et al. (2001) A human mitochondrial ferritin encoded by an intronless gene. J Biol Chem 276:24437–24440

Li RC, Lee SK, Pouranfar F, Brittian KR, Clair HB, Row BW, Wang Y, et al. (2006) Hypoxia differentially regulates the expression of neuroglobin and cytoglobin in rat brain. Brain Res 1096:173–179

Missirlis F, Holmberg S, Georgieva T, Dunkov BC, Rouault TA, Law JH (2006) Characterization of mitochondrial ferritin in Drosophila. Proc Natl Acad Sci USA 103:5893–5898

Nie G, Chen G, Sheftel AD, Pantopoulos K, Ponka P (2006) In vivo tumor growth is inhibited by cytosolic iron deprivation caused by the expression of mitochondrial ferritin. Blood 108:2428–2434

Nie G, Sheftel AD, Kim SF, Ponka P (2005) Overexpression of mitochondrial ferritin causes cytosolic iron depletion and changes cellular iron homeostasis. Blood 105:2161–2167

Nisoli E, Clementi E, Paolucci C, Cozzi V, Tonello C, Sciorati C, Bracale R, et al. (2003) Mitochondrial biogenesis in mammals: the role of endogenous nitric oxide. Science 299:896–899

Santambrogio P, Cozzi A, Levi S, Rovida E, Magni F, Albertini A, Arosio P (2000) Functional and immunological analysis of recombinant mouse H- and L-ferritins from *Escherichia coli*. Protein Expr Purif 19:212–218

Tehranchi R, Invernizzi R, Grandien A, Zhivotovsky B, Fadeel B, Forsblom AM, Travaglino E, et al. (2005) Aberrant mitochondrial iron distribution and maturation arrest characterize early erythroid precursors in low-risk myelodysplastic syndromes. Blood 106:247–253

Valerio A, Cardile A, Cozzi V, Bracale R, Tedesco L, Pisconti A, Palomba L, et al. (2006) TNF-α downregulates eNOS expression and mitochondrial biogenesis in fat and muscle of obese rodents. J Clin Invest 116:2791–2798

Zancani M, Peresson C, Biroccio A, Federici G, Urbani A, Murgia I, Soave C, et al. (2004) Evidence for the presence of ferritin in plant mitochondria. Eur J Biochem 271:3657–3664

The Journal of Histochemistry & Cytochemistry